



## City Research Online

### City, University of London Institutional Repository

---

**Citation:** Tsavdaridis, K. D. & D'Mello, C. (2009). Finite Element Investigation of Perforated Steel Beams with Different Web Opening Configurations. In: Proceedings of Sixth International Conference on Advances in Steel Structures and Progress in Structural Stability and Dynamics. . The Hong Kong Institute of Steel Construction. ISBN 9789889914059

This is the accepted version of the paper.

This version of the publication may differ from the final published version.

---

**Permanent repository link:** <https://openaccess.city.ac.uk/id/eprint/28652/>

**Link to published version:**

**Copyright:** City Research Online aims to make research outputs of City, University of London available to a wider audience. Copyright and Moral Rights remain with the author(s) and/or copyright holders. URLs from City Research Online may be freely distributed and linked to.

**Reuse:** Copies of full items can be used for personal research or study, educational, or not-for-profit purposes without prior permission or charge. Provided that the authors, title and full bibliographic details are credited, a hyperlink and/or URL is given for the original metadata page and the content is not changed in any way.

---

City Research Online:

<http://openaccess.city.ac.uk/>

[publications@city.ac.uk](mailto:publications@city.ac.uk)

---

# **FINITE ELEMENT INVESTIGATION OF PERFORATED STEEL BEAMS WITH DIFFERENT WEB OPENING CONFIGURATIONS**

K. D. Tsavdaridis<sup>1</sup> and C. D'Mello<sup>2</sup>

<sup>1,2</sup> School of Engineering and Mathematical Sciences, City University London,  
Northampton Square, London, U.K.

## **KEYWORDS**

Perforated sections, shear-moment interaction curves, Vierendeel mechanism, non-linear Finite Element Analysis, coupled shear utilisation ratios, plastic hinges, various standard and non-standard web openings

## **ABSTRACT**

The objective of this work is to investigate and compare, through an analytical study, the behaviour of perforated steel beams with different shape configurations and sizes of web openings. In this investigation the 'Vierendeel' failure mechanisms of steel beams with web openings are examined through a Finite Element study. The shear and flexural failures of standard perforated sections are controlled mainly by the size (i.e. depth) of the web openings, whilst the 'Vierendeel' mechanism is primarily controlled by the critical length of the web openings. Three main categories of web opening shape configurations and sizes are considered in this work. Standard, non-standard and elongated web opening configurations are examined, each with three different opening sizes. Four Advanced UB beams are used in the investigation in order to cover a range of sections and demonstrate the main differences in behaviour. The results of this comprehensive FE study are presented and include the position of plastic hinges, the critical opening length of perforated steel sections and the 'Vierendeel' parameters. The yield patterns and the failure modes do not differ dramatically. The results of this study are considered as relevant for practical applications as: (i) the reduction of the moment capacities of the tee-sections due to combination of axial and shear forces is smaller compared to the previous conservative linear interaction formula, and (ii) the formation of the initial plastic hinges at the low moment side (LMS) of the top tee-sections of the web openings does not usually cause failure, meaning that the beams can continue to carry additional load until all four plastic hinges are formed in the vicinity of the web openings and a 'Vierendeel' mechanism is fully established.

## **INTRODUCTION**

The main objective of the work presented here is to investigate the moment-shear (M/V) interaction behaviour of perforated steel beams having different shapes and sizes of web openings. The Finite Element method is used to investigate the behaviour of full scale steel beams with two large isolated openings in the web, symmetrical about the centre-line. To compare the efficiency of the various shapes of web openings, eleven forms are considered, six of these being standard configurations,

including elongated web openings, whilst the other five are elliptical (Figure 1). Web openings C, D, E and F have identical web opening areas, but the last three are rotated by an angle of  $45^\circ$  and hence have a decreased web opening depth. Web opening G is rotated by the same angle but the web opening area is increased and its depth is equal to  $0.8h$  where  $h$  is the depth of the beam. It is well known that the width of the web opening influences the load carrying capacity of the perforated sections and that the critical opening length 'c' is the main dimensional parameter. The associated values of 'c' are listed above the web opening configurations in Figure 1 and in Table 1. Opening depths,  $d_o$ , equal to  $0.8h$ ,  $0.65h$  and  $0.5h$  are investigated.

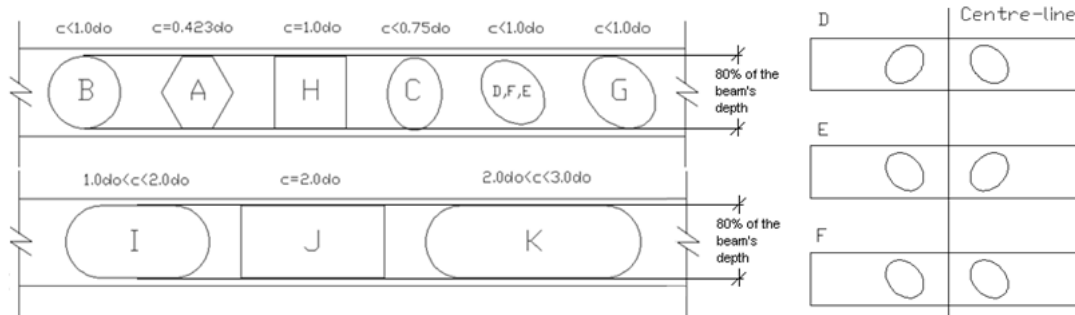


Figure 1: Geometric configurations of web openings (left) and rotated elliptical web openings (right)

Non-linear moment-shear interaction curves are used to present the results of this investigation. A FE model using both geometrical and material non-linearity is used to allow for load redistribution across the web opening following the formation of the first plastic hinge. According to Chung et al. [1] four typical middle-range steel beams commonly used in practice can be investigated in order to obtain useful results. From this work by Chung et al. [1], and from a comprehensive FE analyses conducted by Tsavdaridis [2] on beams UB457x152x52, UB457x152x82, UB610x229x101 and UB610x229x140, beam size UB457x152x52 was selected to represent this study as it produced the most conservative results.

## PARAMETRIC STUDY

### *FEA Model*

In order to simulate the structural behaviour of the perforated sections and investigate the 'Vierendeel' mechanism, a finite element model was established that included both material and geometric non-linearity. The ANSYS four-noded quadrilateral plastic shell element, SHELL181, was used to model the web, flanges and stiffeners. Fine mapped mesh configuration was incorporated in order to avoid discontinuities in stress contours across element boundaries, mainly in the vicinity of the web openings. For the material modelling of steel, a bi-linear stress-strain curve with an elastic modulus,  $E$ , of  $200\text{kN/mm}^2$  and a tangent modulus,  $E_T$ , of  $1000\text{kN/mm}^2$  was adopted, together with a kinematic hardening rule (BKIN) and the Von-Mises yield criteria. The analyses were performed on simply supported beams of 5m span under a uniformly distributed load. Ten different positions of that web

opening along the half length of the beams were considered. The FE model was calibrated against test data, published by Tsavdaridis et al. [3], on a perforated steel I-section with two circular web openings.

### ***Plastic Hinge Positions***

Von-Mises stresses are used to reveal the plastic hinges in the vicinity of the web openings which are formed at both ends of the tee-sections. The positions of these plastic hinges are influenced by the magnitude of the global shear force and bending moment. The shear forces produce additional moments ('Vierendeel' action), as first mentioned by Bower [4] and Redwood [5]. By understanding the movement and the critical positions of these plastic hinges, the actual critical opening length can be obtained. Figure 2 shows these hinge positions for different web opening shapes for section UB457x152x52, with web openings of depth equal to 0.8h and at a distance, x, of 0.284m from support.

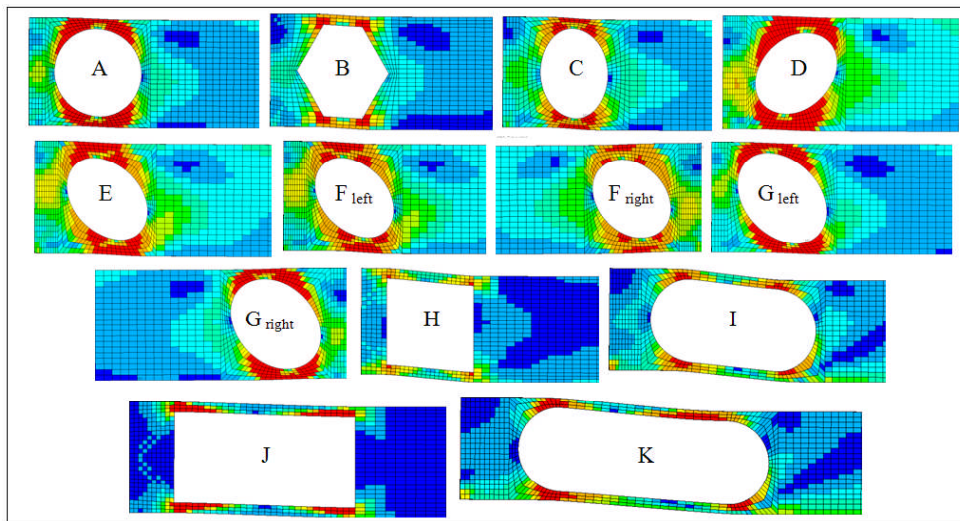


Figure 2: Von-Mises stresses of beams subjected to high shear forces

This FE study found that in the case of non-standard web openings, the structural performance of the perforated sections is strongly affected by not only by the opening depth and critical length, but also the web opening shape. In perforated sections with elliptical web opening configurations, the yield zones overlapped significantly when the web opening positions were changed. Generally, it can be concluded that in terms of stress distribution, perforated sections with vertical and rotated elliptical web openings have a better performance compared to circular and hexagonal web openings. This was expected, especially for vertical elliptical web openings, as the web opening width is narrower.

### ***Moment /Shear (M/V) Interaction Curves***

A practical design method proposed by Chung et al. [6], is related to 'coupled' shear capacities and allows for the 'Vierendeel' mechanism. The behaviour of perforated sections is characterized by three actions: global bending action, global shear action and local 'Vierendeel' action. The moment shear interaction curves obtained from the finite element investigation are presented in Figure 3, where the

vertical axis is the ‘coupled’ shear ratio and the horizontal axis is the moment ratio. At failure, the global shear force,  $V_{o,Sd}$  (Eqn. 1) and the global moment,  $M_{o,Sd}$ , (Eqn. 2) at the centre-line of the openings, are non-dimensionalised with respect to the global section capacities of the perforated sections,  $V_{o,Rd}$  and  $M_{o,Rd}$ , Eqn. 3 and Eqn. 4, respectively. All interaction curves are generally similar in pattern and therefore allow for an application of a generalized M/V interaction curve for practical design. It is worth noting that the reduction in the shear capacity is more pronounced when compared to the reduction in the moment capacity, as the presence of the opening in the web reduces the shear area of the section significantly whilst the reduction of the bending modulus is small. The moment utilisation ratio is sometimes greater than one, whereas in other cases remarkable reduction of the moment capacity is also obtained.

$$V_{o,Sd} = w \left( \frac{L}{2} - x \right) \quad (1)$$

$$M_{o,Sd} = wx \frac{(L-x)}{2} \quad (2)$$

$$V_{o,Rd} = f_v A_{vo} \geq V_{Sd}, \quad A_{vo} = A_v - d_o t_w, \quad f_v = \frac{0.577 f_y}{\gamma_{Mo}} \quad (3)$$

$$M_{o,Rd} = f_y W_{o,pl} \geq M_{Sd}, \quad W_{o,pl} = W_{pl} - \frac{d_o^2 t_w}{4} \quad (4)$$

Where  $w$  is the failure load from the FE model, (N/mm),  $L$  is the span of the specimen (5000mm),  $x$  is the web opening positions along the beam,  $E$  is the Young’s Modulus of the steel beam (200kN/mm<sup>2</sup>),  $I$  is the Second Moment of Area of the un-perforated steel beam (21369E4mm<sup>4</sup>),  $W_{pl}$  is the plastic modulus of the overall section,  $t_w$  is the web thickness,  $d_o$  is the diameter of the web opening,  $f_y$  is the design yield strength of the steel (275N/mm<sup>2</sup>),  $f_v$  is the shear strength of the steel,  $A_v$  is the shear area of the un-perforated section and  $h$  is the overall depth of the steel beam.

Perforated sections with elliptical web openings generally behave similarly to the other web opening configurations. However, from the FE analysis, it was found that as the web opening size increased the utilisation ratios of the perforated sections also increased. Most affected are the perforated sections with web openings of  $d_o$  equal to 0.5h, where both the x- and y-intercepts are significantly reduced and an uneven stress distribution is observed. The rotation of the elliptical web openings is a key parameter. By rotating all sizes of web openings 45° to the vertical centre-line of the web opening, a reduction of depth of around 11.5% is obtained. However, this dissimilarly affects the design capacity values,  $V_{o,Rd}$  and  $M_{o,Rd}$ . Consequently, regarding the standard web openings it can be concluded that the bigger the web opening size the higher the reduction of the utilisation ratio is.

Investigating the perforated sections with inclined web openings G with  $d_o$  equal to 0.8h, 0.65h and 0.5h, it can be seen that the utilisation ratios for all three web opening sizes are close to each other and the overall behaviour is similar to the other sections with elliptical web openings. Even though web opening G has only a 3.7% smaller web opening area than web opening A, the M/V curves are quite different. This is due to shift of the stress concentration points, where the web opening shape and opening length controls their behaviour. Overall, it can be concluded that when perforated sections with elliptical web openings are used, the opening length of the web openings is the main parameter.

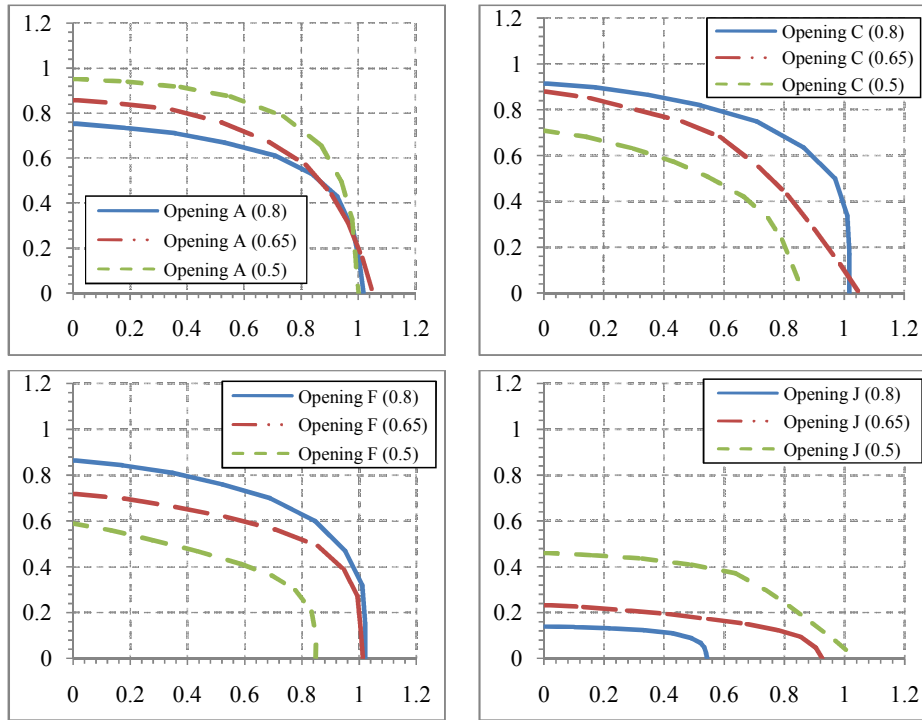


Figure 3: M/V interaction curves for various web opening configurations obtained from FEA

TABLE 1  
SUMMARY OF COUPLED SHEAR RATIOS FOR PERFORATED SECTIONS WITH WEB OPENINGS OF VARIOUS SHAPES AND SIZES

| Opening Types           | Opening Shapes | Opening Length, c | 'Coupled' Shear Ratios |      |       |       |      |      |
|-------------------------|----------------|-------------------|------------------------|------|-------|-------|------|------|
|                         |                |                   | 0.44h                  | 0.5h | 0.57h | 0.65h | 0.7h | 0.8h |
| Standard Typical        | A              | 0.23              | N.A.                   | 0.95 | N.A.  | 0.86  | N.A. | 0.75 |
|                         | B              | 0.43              | N.A.                   | 0.92 | N.A.  | 0.82  | N.A. | 0.65 |
| Non-Standard Elliptical | C              | 0.14              | N.A.                   | 0.71 | N.A.  | 0.88  | N.A. | 0.92 |
|                         | D              | 0.25              | 0.60                   | N.A. | 0.79  | N.A.  | 0.88 | N.A. |
|                         | E              | 0.25              | 0.59                   | N.A. | 0.78  | N.A.  | 0.87 | N.A. |
|                         | F              | 0.25              | 0.59                   | N.A. | 0.72  | N.A.  | 0.87 | N.A. |
|                         | G              | 0.21              | N.A.                   | 0.71 | N.A.  | 0.79  | N.A. | 0.74 |
| Standard Elongated      | H              | 1.00              | N.A.                   | 0.65 | N.A.  | 0.48  | N.A. | 0.26 |
|                         | I              | 1.16              | N.A.                   | 0.56 | N.A.  | 0.35  | N.A. | 0.22 |
|                         | J              | 2.00              | N.A.                   | 0.46 | N.A.  | 0.23  | N.A. | 0.14 |
|                         | K              | 2.23              | N.A.                   | 0.37 | N.A.  | 0.20  | N.A. | 0.13 |

Table 1 summarizes the values of the 'coupled' shear ratios, for perforated sections obtained from the comprehensive finite element investigation of the current study. 'Coupled' capacities are found to depend not only on the shapes and sizes of web openings, but also on the applied global shear forces

and moments. Hence, the position of the web opening as well as the loading arrangement affects the ‘coupled’ shear capacities.

### ***Moment/Shear Ratios for Various Section Sizes***

From the FE analysis, it is found that in an I-section with large web openings the shear area of the web is significantly reduced, and hence the shear areas of the flanges are taken into consideration in assessing the shear capacity of the perforated section [6]. Hence, in the aforementioned FE analyses the following assumption, presented in Eqn. 5, is utilised. Table 2 presents the differences by using the latter assumption and the ones based on simple plastic section analysis, where the shear area of an I-section is taken either as  $h \times t_w$  for practical reasons, or as given in Eqn. 6 below, from in ENV (1993-1-3) EC3 [7].

$$A_v = ht_w + 2(0.75t_f^2) \quad (5)$$

$$A_{vz} = A - 2bt_f + (t_w + 2r)t_f \quad (6)$$

For beam sections with thick flanges, the increase in shear capacities can exceed 30%. This percentage is decreased for perforated sections with smaller web opening sizes. Also, the  $t_w/h$  ratio affects the bending capacity of the perforated sections to a lesser extent.

Table 2 presents the ‘coupled’ shear ratios from the present FE study for one web opening of each category according to the aforementioned assumptions, together with the percentage differences between them. The Eqn. 5 shows a greater decrease of the utilisation factor when UB 457x152x52 sections are investigated. It is seen that both the  $t_f$  and  $t_w$  parameters are considered, although  $t_f$  is generally domain.

### ***‘Vierendeel’ Parameter***

The ‘Vierendeel’ moment across the opening is resisted by the plastic moment capacities of the sections, which may or may not be stiffened. For beams with circular openings Redwood [8] proposed an effective size of rectangular opening. A ‘Vierendeel’ parameter,  $v_i$ , is used for this purpose and is defined in Eqn. 7 [6].

$$v_i = \frac{V_{o,Rd,Vi}}{\frac{4M_{T,Rd}}{c}} \quad (7)$$

Where  $M_{T,Rd}$  is the basic shear capacity of the tee-sections under zero axial and shear forces,  $V_{o,Rd,Vi}$  is the global ‘coupled’ shear capacity of perforated sections as obtained from FEA, and  $c$  is the critical opening length.

Figure 4 shows typical values of the ‘Vierendeel’ mechanism for perforated sections under zero global moment. The results show that the ‘Vierendeel’ parameter increases as the critical opening length is increased and tends towards unity, thus illustrating the importance of the ‘Vierendeel’ mechanism.



TABLE 2  
COUPLED SHEAR RATIOS OF TEE-SECTIONS

| Section Sizes     | Opening Shape | Opening Size $d_o/h$ | $t_f/t_w$ | $t_w/h$ | $h_x t_w$ ratio | EC3 Eqn. 6 ratio | [5] Eqn. 5 ratio | $h_x t_w$ Vs. EC3 (%) | $h_x t_w$ Vs. [5] (%) |
|-------------------|---------------|----------------------|-----------|---------|-----------------|------------------|------------------|-----------------------|-----------------------|
| UB<br>610x229x140 | A             | 0.8                  | 1.69      | 0.0212  | 1.11            | 0.90             | 0.77             | 18.9                  | 30.6                  |
|                   | C             |                      |           |         | 1.47            | 1.17             | 1.02             | 20.4                  | 30.6                  |
|                   | I             |                      |           |         | 0.76            | 0.62             | 0.53             | 18.4                  | 30.3                  |
| UB<br>610x229x101 | A             | 0.8                  | 1.41      | 0.0174  | 0.96            | 0.76             | 0.78             | 20.8                  | 18.8                  |
|                   | C             |                      |           |         | 1.27            | 0.98             | 1.01             | 22.8                  | 20.5                  |
|                   | I             |                      |           |         | 0.47            | 0.39             | 0.39             | 17.0                  | 17.0                  |
| UB<br>457x152x82  | A             | 0.8                  | 1.80      | 0.0225  | 1.17            | 0.93             | 0.77             | 20.5                  | 34.2                  |
|                   | C             |                      |           |         | 1.42            | 1.12             | 0.93             | 21.1                  | 34.5                  |
|                   | I             |                      |           |         | 0.77            | 0.60             | 0.44             | 22.1                  | 42.8                  |
| UB<br>457x152x52  | A             | 0.8                  | 1.43      | 0.0168  | 0.95            | 0.72             | 0.75             | 24.2                  | 21.0                  |
|                   | C             |                      |           |         | 1.16            | 0.87             | 0.92             | 25.0                  | 20.7                  |
|                   | I             |                      |           |         | 0.27            | 0.20             | 0.22             | 25.9                  | 18.5                  |

**Position of First Plastic Hinge**

Non-linear FE analyses have shown that failure is dominated by web post for low axial force in the tee-section, and ‘Vierendeel’ for high axial force in the tee-section. Curved beam theories by Olander [9] and Sahmel [10] were used in order to assess the results. The overall view is that as the angle  $\phi_p$  of the plastic hinge is increased, the ratio of axial force to shear force also increases.

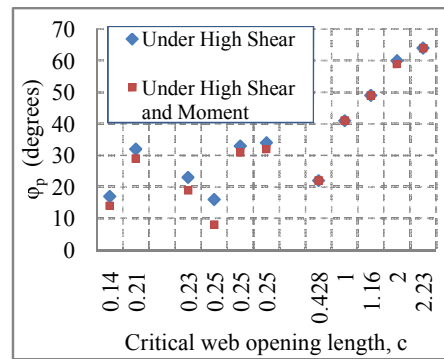
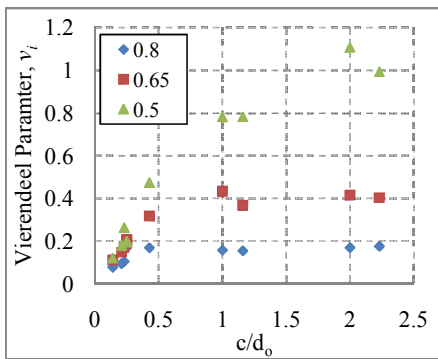


Figure 4: Typical values for ‘Vierendeel’ parameter      Figure 5:  $\phi_p$  values of the first plastic hinge

The angle  $\phi_p$  of the first plastic hinge always occurs at the LMS of the top tee-section. After the formation of the first plastic hinge, there is load redistribution across the web opening and the plastic hinges are formed in a slightly different way. Typically, the larger the opening length,  $c$ , the higher the  $\phi_p$  value is. However, as it shown from Figure 5 the shape of the web opening also significantly affects the position of the plastic hinges. Furthermore, it can be concluded that in perforated sections with polygonal web openings, the stress usually tends to concentrate at the sharp corners of the polygons. Also, it should be clearly stated that perforated sections with non-standard elliptical web openings

behave similarly to the standard non-polygon web openings in terms of the sequence of the plastic hinges formation, independent of the web opening shape.

## CONCLUSIONS

Finite element analyses of perforated sections with different standard and non-standard web opening configurations show how the 'Vierendeel' mechanism is affected by the shapes and sizes of the web openings. The investigation on novel elliptical web openings presents some new results and others that update current knowledge. The FE analysis provides a good prediction of the 'Vierendeel' loads but the results are more applicable if calibrated against other FEA results found in the literature and/or against experimental work with similar test configurations. The effects of the flange and web thicknesses, as well as the critical web opening length and depth are presented herein through a comprehensive parametric FE investigation.

## REFERENCES

- [1] Chung K.F., Liu T.C.H. and Ko A.C.H., "Investigation on Vierendeel mechanism in steel beams with circular web openings", *Journal of Constructional Steel Research*, 2001, 57, pp.467-490
- [2] Tsavdaridis, K. D., "Failure modes of composite and non-composite perforated beams sections with various shapes and sizes of web openings", PhD thesis in preparation (supervised by Dr. C. D'Mello), School of Engineering and Mathematical Sciences, City University, London, 2010
- [3] Tsavdaridis, K.D., D'Mello, C. & Hawes, M., "Experimental study of ultra shallow floor beams with perforated steel sections", 11<sup>th</sup> Nordic Steel Construction Conference (Malmö Sweden September 2-4, 2009) NSCC2009 Press, Malmö, Sweden, 2009
- [4] Bower J. E., "Design of beams with web openings", *Journal of the Structural Division, Proceedings of the American Society of Civil Engineers*, 1968
- [5] Redwood R.G., "The strength of steel beams with unreinforced web holes", *Civil Engineering and Public Works Review*, 1969
- [6] Chung K.F., Liu T.C.H. and Ko A.C.H., "Steel beams with large web openings of various shapes and sizes: an empirical design method using a generalized moment-shear interaction", *Journal of Constructional Steel Research*, 2003, 59, pp.117-1200
- [7] ENV 1993-1-3, Eurocode 3: Design of steel structures: Part1.1. General rules and rules for buildings, 1992, and Amendment A2 of Eurocode 3: Annex N 'Openings in webs'. British Standards Institute, 1998
- [8] Redwood R.G., "Design of beams with web holes", Canadian Steel Industry Construction Council, Willowdale, Ontario, Canada, 1973
- [9] Olander H.C., "A method of calculating stress un rigid frame corners", *Journal of ASCE*, August 1953
- [10] Sahlmeier P., "The design construction and approximate calculation of welded transverse beams and torsion bars having pronounced web clearance", *Schweissen und Schneiden*, No.4